

Caloric restriction reduces edema and prolongs survival in a mouse glioma model

Yong-Sheng Jiang · Fu-Rong Wang

Received: 17 September 2012 / Accepted: 12 May 2013 / Published online: 24 May 2013
© Springer Science+Business Media New York 2013

Abstract Regardless of their cell type of origin, all aggressive brain tumors, such as malignant gliomas and metastatic tumors produce brain edema, which is an important cause of patient morbidity and mortality. Caloric restriction (CR) has long been recognized as a natural therapy that improves health, promotes longevity, and significantly reduces both the incidence and growth of many tumor types. The aim of present work was to investigate the effect of CR on edema and survival in the mice implanted with U87 gliomas. We found that CR significantly inhibited the intracerebral tumor growth, attenuated brain edema, and ultimately prolonged survival of mice with U87 gliomas. Plasma corticosterone level was found higher and serum VEGF and IGF-1 levels were found lower in CR, when compared to AL group. CR upregulated tight junction proteins including claudin-1, claudin-5 and ZO-1, downregulated VEGF and VEGFR2, enhanced α -SMA expression, and reduced AQP1 expression in U87 gliomas. In addition, CR suppressed inducible nitric oxide synthase (iNOS) expression and nitric oxide (NO) formation in U87 gliomas. In conclusion, CR attenuated edema in U87 orthotopic

mouse glioma model associated with elevation of corticosterone, suppression of VEGF/VEGFR2, improvement of tight junctions, and suppression of iNOS expression and NO formation. Our results suggested that CR might be an effective therapy for recurrent malignant brain cancers through alleviating associated edema.

Keywords Caloric restriction · Edema · Glioma · Permeability

Introduction

Patients with high grade gliomas typically have a poor prognosis, even after aggressive surgery, radiation and advanced chemotherapy. Cerebral edema, a common occurrence in patients with gliomas, is a frequent cause of morbidity and mortality. In fact, clinical deficits are more often caused by edema rather than by mass effects of tumors [1, 2]. Although treatment with corticosteroids results in dramatic clinical improvement of edema, their use is often associated with detrimental side effects, especially at high doses and long-term administration [3, 4]. New strategies are required for the treatment of edema induced by gliomas.

Caloric restriction (CR) is produced from a total restriction of dietary nutrients and differs from starvation in that CR reduces total caloric energy intake without causing anorexia or malnutrition [5]. In recent years, CR has been studied intensively with consistent results showing its beneficial effects on longevity, age-associated diseases and carcinogenesis across a variety of species [6–8]. Multiple mechanisms of action might be involved in the anti-tumorigenic effect of CR. Reports about gliomas demonstrated that CR could suppress tumor growth [9], enhance

Electronic supplementary material The online version of this article (doi:10.1007/s11060-013-1154-y) contains supplementary material, which is available to authorized users.

Y.-S. Jiang
Center of Tumor, Tongji Hospital of Tongji Medical College,
Huazhong University of Science and Technology, Wuhan,
People's Republic of China

F.-R. Wang (✉)
Department of Neurology, Tongji Hospital of Tongji Medical
College, Huazhong University of Science and Technology,
1095 Jiefang Road, Wuhan 430030,
People's Republic of China
e-mail: jiangyongsheng2012@hotmail.com

vessel maturation [10], reduce angiogenesis [11], enhance apoptosis [12], and decrease invasive property [13]. However, whether CR could attenuate edema induced by gliomas remained unknown. Considering the important role of edema in gliomas, the aim of present work was to elucidate the effect of CR on edema in U87 gliomas.

Materials and methods

Chemicals

Unless otherwise specified, reagents were purchased from Sigma-Aldrich (St Louis, MO).

Animals

Male athymic mice (9–10 week-old) were purchased from Vital-Aiver Animal Ltd (Beijing, China). All the mice were entrained to controlled temperature (23–25 °C), 12-h light and 12-h dark cycles (light, 08:00–20:00 h; darkness, 20:00–08:00 h). All the mice used in this work received humane care in compliance with institutional animal care guidelines, and were approved by the Local Institutional Committee. All experimental procedures were in accordance with institutional animal care guidelines.

The mice were group housed prior to the initiation of the experiment and were then housed singly 1 day before tumor implantation. 2 days after tumor implantation, animals were randomly divided into AL (95 % of average daily intake) or CR (60 % average daily intake) groups. According to the manufacturer's specification, the diet used in the experiments delivered 4.4 kcal/g gross energy, where fat, carbohydrate, protein, and fibre comprised 55, 520, 225, and 45 g/kg of the diet, respectively. All animal were given free access to water throughout the experiment.

Mouse brain tumor model

U87 human glioma cells were grown in monolayer culture in Dulbecco's modified Eagle's medium supplemented with 10 % fetal bovine serum and antibiotics. Cells were harvested immediately prior to intracerebral implantation in mice and were used only if viability exceeded 90 %. Injections consisted of 5 μ l of a cell suspension containing 2×10^6 to 5×10^6 cells/ μ l implanted with a 28-gauge microsyringe. Injections were performed with the mouse head fixed in a stereotaxic device (Small Animal Stereotaxic Instrument with Mouse Adaptor, David Kopf Instruments, CA). The needle tip was positioned at an angle of 55° and depth of 1.75 mm, and cells were injected slowly over 1 min. This injection technique ensures implantation of a sufficient number of cells into the superficial mouse brain

cortex. U87 tumors implanted in the brain were firm nodular masses, and easily dissected. When the arising tumor reached approximately 3×3 mm, it was harvested and divided into small fragments ($\sim 0.2 \times 0.3$ mm). The tumor fragments were implanted into the mice by dissecting the skin from a small area of the skull and drilling a hole, slightly anterior to the bregma and lateral to the midline. A small portion of tumor tissue was implanted with a 30-gauge needle in the exposed brain. Initiation of tumors from intact tumor pieces was preferable to initiation from cultured cells because the pieces already contained an established micro-environment that facilitated tumor growth [14].

Two days after implantation, mice were provided with food either ad libitum (AL) or under caloric restriction (CR).

Measurement of glucose, lactate, corticosterone and β -OHB in plasma and IGF-1 and VEGF in serum

All mice were fasted for 3 h before blood collection. The mice were anaesthetised, and blood was collected for analysis of several biomarkers.

Plasma glucose and β -hydroxybutyrate (β -OHB) concentrations were measured spectrophotometrically using the Trinder assay and a UV enzymatic assay, respectively.

Plasma lactate levels were measured with a commercial Lactate Assay kit (K607-100, BioVision, Inc., San Francisco, USA).

Plasma corticosterone levels were measured with a Corticosterone EIA Kit (Cayman, Michigan, USA).

Serum IGF-1 and VEGF levels were evaluated using enzyme-linked immunosorbent assay (ELISA) kits (R&D Systems, Minneapolis, MN, USA).

Regional tumor permeability study

Quantitative autoradiography for the assessment of vascular permeability was performed by determining the blood-to-tissue transfer constant K_i as described previously [15]. The permeability tracers [14 C] AIB (MW 100) and [14 C] sucrose (MW 372) were given as an i.v. bolus (80 mCi). Arterial blood samples were taken at selected intervals, and plasma radioactivity was determined by liquid scintillation counting with appropriately quenched [14 C] standards. After 15 min, the mice were decapitated, and the brains were rapidly removed and frozen in isopentane on dry ice. Tissue sections were serially sliced in 20 μ m sections throughout the whole tumor area on a cryostat. The sections were thawed and mounted onto slides, and autoradiographs were generated by exposing the sections along tissue-calibrated 14 C standards on a phosphor screen for 5 days. Quantitative analysis of the regional radioactivity for tumor center was done using the Image 1.55 software

(NIH). The initial rate for blood-to-brain transfer (K_i) was calculated as described [16].

Magnetic Resonance Imaging (MRI)

MRI T2 relaxation map was performed 14 days after tumor implantation. All MR images were acquired using a 9.4 Tesla MRI scanner (Magnex Scientific Ltd, Oxford, UK). Mice were positioned on a custom made mouse cradle and anesthetized with a 50/50 mixture of O₂ and medical air plus 1.5 % isoflurane and placed prone in a home-built cradle. A custom-built transmit-receive birdcage mouse-head coil was used to acquire the images. T2 relaxation maps were generated from multi-echo spin-echo images and used to assess tumor edema. Acquisition parameters were: TE = 10 ms, 10 echoes, TR = 2500 ms, 11 image slices, 0.5 mm slice thickness, 150 μm in-plane resolution, NA = 2. Voxelwise exponential fitting of the image signal intensity as a function of echo-time was performed using a MATLAB program written in-house to determine T2 relaxation time maps.

Western blotting analysis

The protein concentration was determined with bovine serum albumin as a standard by a Bradford assay. Equal amount of protein preparations (10 μg in 10 μl buffer) were run on SDS–polyacrylamide gels, electrotransferred to polyvinylidene difluoride membranes, and incubated with primary antibodies against AQP1, AQP4, VEGF, VEGFR2, α-SMA, claudin-1, claudin-5, ZO-1, iNOS, occludin, p53, cyclin D1, bax, bcl-2, beclin-1 and Atg5 (Santa Cruz, CA, USA) overnight at 4 °C using slow rocking. Then, they were incubated with HRP-conjugated secondary antibody. Immunoreactive bands were detected by a chemiluminescent reaction (ECL kit, Amersham Pharmacia, CA, USA), and results were expressed as the ratio of the density of specific bands to the corresponding β-actin. The AL group was used as the calibrator with a given value of 100 %, and the other groups were normalized with this calibrator.

Measurement of nitrate and nitrite in tumor tissues

The final products of NO in vivo are nitrite (NO₂⁻) and nitrate (NO₃⁻). Sum of nitrate and nitrite is an index of total NO production. Nitrate and nitrite were measured by using a fluorometric assay kit (Cayman Chemical, Michigan, USA).

Water content analysis by dry/wet weight measurements

Anesthetized mice were euthanized by cervical dislocation and the brains were collected. Brains were dissected into

several compartments: tumor, ipsilateral hemisphere, and contralateral hemisphere. Tissues were weighed immediately and dried in a vacuum for up to 2 weeks. Weights were collected throughout the drying period until the final dry weight was established. Water content was calculated as follows: Water content = (wet weight-dry weight)/wet weight

Study design

Experiment 1: we implanted small fragments (0.2–0.3 mm diameter) of U87 into brain. 2 days later, animals were randomly divided into AL or CR groups (n = 23 in each group). 14 days after tumor implantation, MRI T2 relaxation map was performed; blood was collected for determination of glucose, lactate, β-OHB, VEGF, IGF-1 and corticosterone. Tumor was removed for evaluation of tumor growth, edema and tumor permeability and assessment of protein expressions including VEGF, claudin-1, occludin, AQP1, iNOS and AQP4 and levels of nitrate and nitrite in tumor tissues.

Experiment 2: we implanted small fragments of U87 into brain. 2 days after implantation, animals were randomly divided into AL or CR groups (n = 7 in each group) and the overall survival was observed in two groups. For experimental assessment of survival, all animals were killed when they lost 20 % of their body weight or had difficulty ambulating, feeding, or grooming.

Statistical analysis

All data except overall survival are expressed as mean ± SD. The principal statistical test was the *t* test (Student's *t* test with unequal variance). Survival was estimated using the Kaplan–Meier product limit method, and differences among the groups were assessed with the generalized Wilcoxon test. *P* < 0.05 was considered statistically significant. Statistical analysis was performed using SPSS 11.0.0 software (SPSS Inc., Chicago, IL, USA).

Results

Influence of CR on body weight, tumor growth, and several biomarkers in plasma and serum of mice with U87 gliomas

Caloric restriction resulted in a progressive reduction in the average body weight between 3 and 14 days after tumor implantation. The average body weight for the CR group was 23.9 % less than that for the AL group on the 14 day after tumor implantation (Fig. 1a, *p* < 0.05). Despite a

reduction in total body weight, the CR mice seemed healthy and were more active than the AL mice as assessed by ambulatory and grooming behavior. No signs of vitamin or mineral deficiency were observed in the CR mice according to standard criteria for mice [17]. These findings are consistent with the well-recognized health benefits of diet restriction in rodents [18, 19].

14 days after tumor implantation, U87 tumor weight was 51 % less in the CR group than that for AL group (Fig. 1b, $p < 0.05$), indicating that CR significantly suppressed tumor growth.

Blood was collected 14 days after tumor implantation. CR significantly reduced plasma levels of glucose (Fig. 1c, $p < 0.05$), and decreased serum levels of IGF-1 (Fig. 1f, $p < 0.05$) and VEGF (Fig. 1g, $p < 0.05$), and enhanced plasma levels of β -OHB (ketone body, Fig. 1e) and corticosterone (Fig. 1h, $p < 0.05$). CR led to a reduction in plasma lactate (Fig. 1d, $p = 0.087$), but not significantly.

CR upregulated p53 expression ($p < 0.05$) and downregulated cyclin D1 expression ($p < 0.05$) in U87 gliomas (Supplementary Fig. 1a, b), indicating that CR could arrest cell cycle of glioma cells. CR upregulated bax expression

($p < 0.05$) and downregulated bcl-2 expression ($p < 0.05$) in U87 gliomas (Supplementary Fig. 1a, c), indicating that CR could promote apoptosis in gliomas. CR upregulated beclin-1 ($p < 0.05$) and Atg5 ($p < 0.05$) in U87 glioma (Supplementary Fig. 1a, d), indicating that CR could induce autophagy of glioma cells.

Influence of CR on tumor permeability and edema of mice with U87 gliomas

Permeability analysis was performed 14 days after tumor implantation. CR decreased the [14 C] AIB (Fig. 2a, $p < 0.05$) and [14 C] sucrose (Fig. 2b, $p < 0.05$) uptakes by the tumors, indicating that CR led to a significant reduction in permeability of U87 gliomas.

The decreased T2 observed after dietary treatment was significantly different from the increased T2 observed in AL mice (Fig. 2c, $p < 0.05$). The result of MRI analysis indicated that CR reduced edema in U87 gliomas.

14 days after implantation, the brains were removed for edema analysis. CR decreased water content of tumor (Fig. 2d, $p < 0.05$) and ipsilateral cerebrum (Fig. 2e,

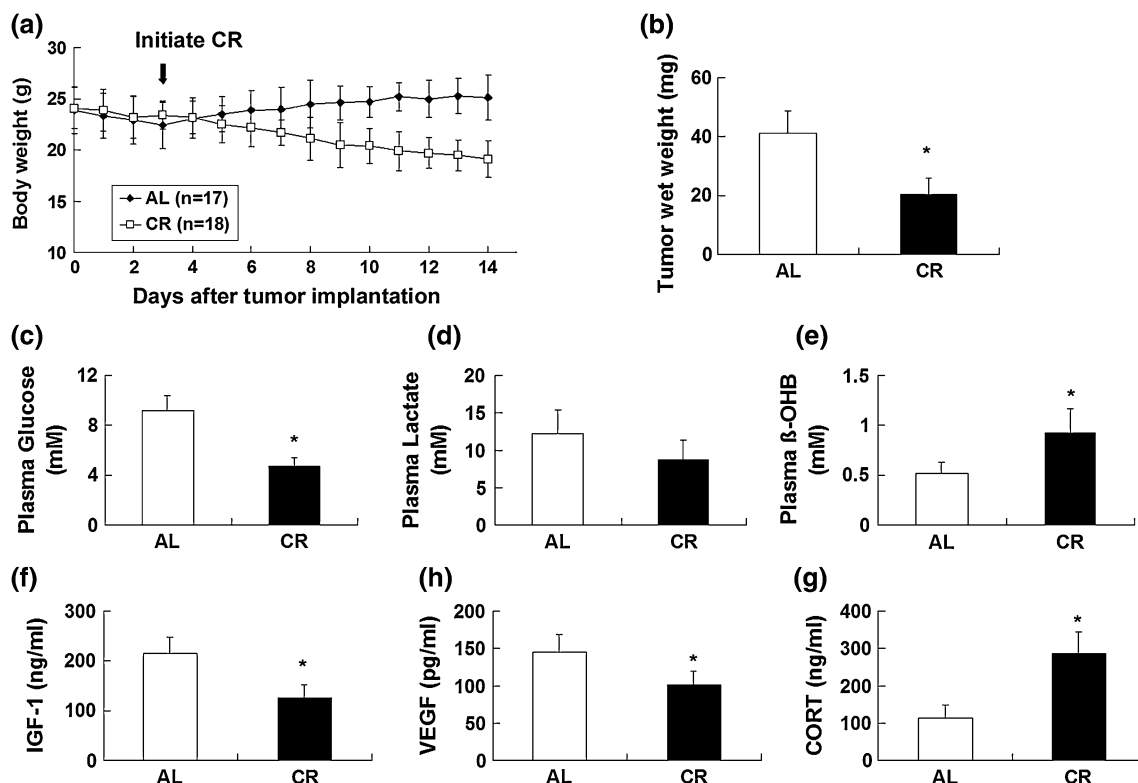


Fig. 1 Influence of CR on body weight, tumor growth, and several biomarkers in plasma and serum of mice with U87 gliomas. Dietary treatment was started 2 days after tumor implantation. Body weight (a) was recorded every day. 14 days after tumor implantation, U87 gliomas were removed and weighted (b); the levels of glucose (c), lactate (d), β -OHB (e), and corticosterone (h) were determined in

plasma; the levels of IGF-1 (f) and VEGF (g) were determined in serum. $n = 17$ in AL group; $n = 18$ in CR group; VEGF, vascular endothelial growth factor; IGF-1, insulin-like growth factor 1; β -OHB, β -hydroxybutyrate; CORT, corticosterone; * $p < 0.05$ versus AL group

$p < 0.05$) significantly, but had no significant effect on water content of contralateral cerebrum (Fig. 2f). This result further demonstrated that CR reduced edema produced by implanted U87 gliomas.

Influence of CR on survival of mice with U87 gliomas

According to Kaplan–Meier analysis, the survival curves for the AL and CR mice differed significantly. CR markedly prolonged the survival (Fig. 3, $p < 0.05$) of U87-inoculated mice when compared to AL group.

Influence of CR on proteins expression in U87 gliomas

Tumors were removed for Western blotting analysis 14 days after tumor implantation.

CR upregulated proteins expression of claudin-1 ($p < 0.05$), claudin-5 ($p < 0.05$) and ZO-1 ($p < 0.05$), indicating that CR could improve tight junctions of vessel in U87 gliomas. But, CR had no significant effect on occludin expression in U87 gliomas (Fig. 4a, b).

CR reduced AOP1 protein expression ($p < 0.05$), but had no significant effect on AQP4 protein expression (Fig. 4a, c).

CR suppressed proteins expression of VEGF ($p < 0.05$) and VEGFR2 ($p < 0.05$), indicating that CR suppressed VEGF/VEGFR2 pathway in U87 gliomas. CR upregulated protein expression of α -SMA (a marker of pericyte, $p < 0.05$), indicating that CR could promote vessel maturation in U87 gliomas (Fig. 4a, d).

CR downregulated iNOS expression ($p < 0.05$) and reduced NO formation ($p < 0.05$) in U87 gliomas (Fig. 4a, e, f), indicating that CR could suppress iNOS/NO pathway in U87 gliomas.

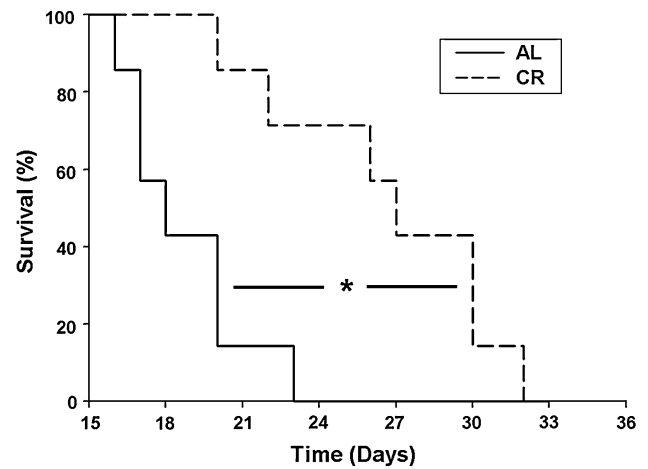


Fig. 3 Influence of CR on survival of mice with U87 gliomas. Overall survival was calculated from the day of inoculation to end of survival. Survival was estimated using the Kaplan–Meier product limit method. $n = 7$ in each group; $*p < 0.05$ versus AL group

Discussion

Different from normal brain tissue that can derive energy from both glucose and ketone bodies, most tumors including gliomas lack metabolic versatility and are dependent largely on glucose for energy [20, 21]. In this work, CR significantly reduced plasma glucose and suppressed glycolysis, as indicated by a reduction of plasma lactate; CR increased production of ketone bodies, as indicated by an increase of β -OHB. Seyfried et al. found that reduction of plasma glucose together with elevation of plasma ketones were associated with the anti-tumor efficacy of CR [9]. In this work, CR suppressed tumor growth, which was consistent with previous report [9]. Our results revealed that CR arrested cell cycle, promoted apoptosis,

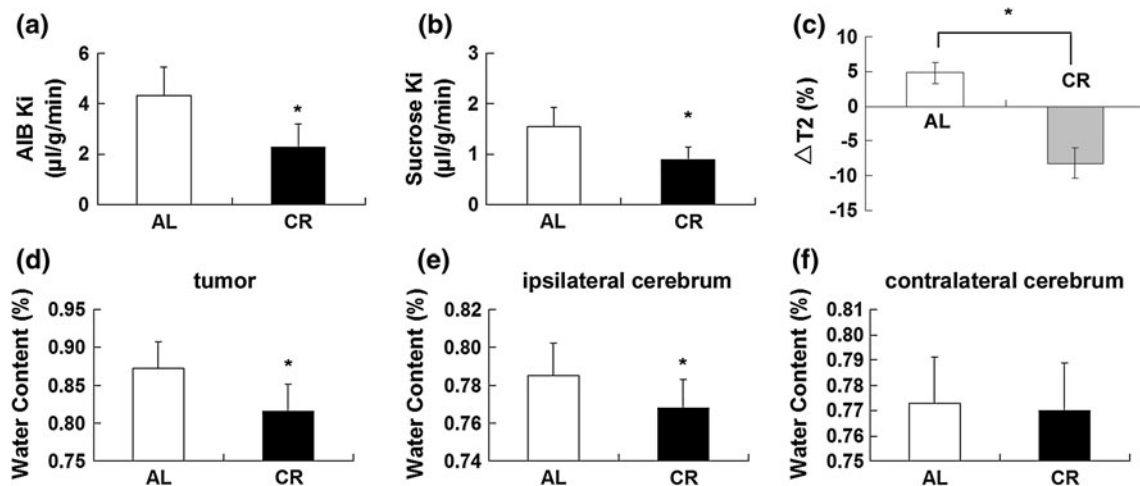


Fig. 2 Influence of CR on tumor permeability and edema of mice with U87 gliomas. 14 days after tumor implantation, tumor permeability (a, b), tumor edema (c), and water content (d, e, and f) in tumors and brains were determined. $n = 7$ in each group. $*p < 0.05$ versus AL group

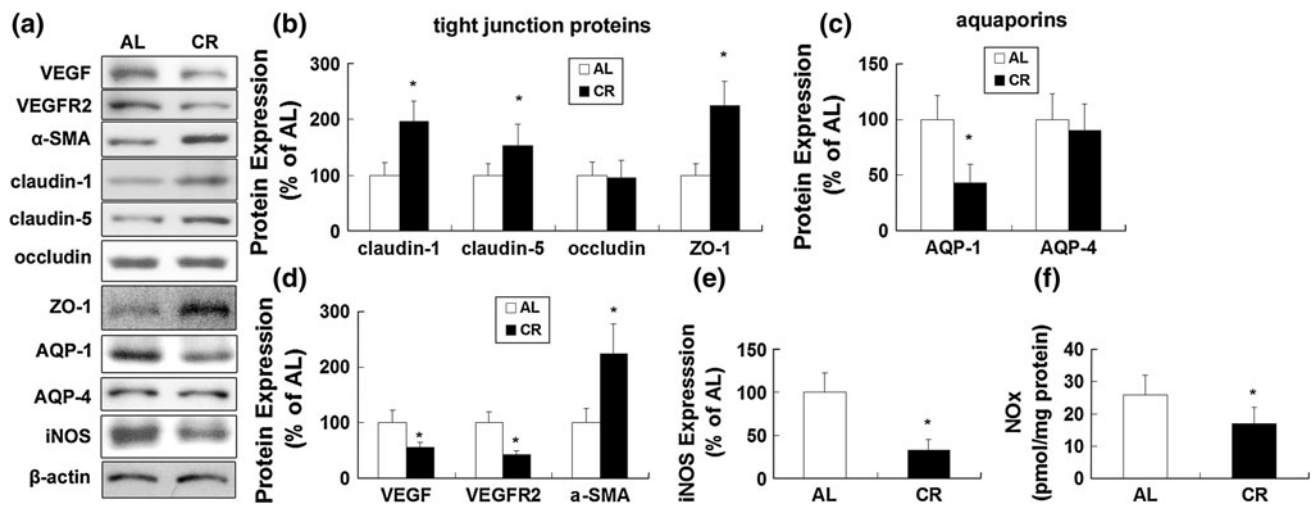


Fig. 4 Influence of CR on proteins expression of VEGF, VEGFR2, α -SMA, claudin-1, claudin-5, occludin, ZO-1, iNOS, AQP1 and AQP4 in U87 gliomas. 14 days after tumor implantation, tumors were removed for determination of protein expression of VEGF, VEGFR2, α -SMA, claudin-1, claudin-5, occludin, ZO-1, AQP1 and AQP4 by Western blotting analysis (a). Graphs showed the responding quantification of these proteins (b, c, d, and e). 14 days after tumor

implantation, tumors were removed for determination of NOx (f, $\text{NO}_2^- + \text{NO}_3^-$) content. $n = 7$ in each group in the measurement of NOx; VEGF, vascular endothelial growth factor; VEGFR2, vascular endothelial growth factor receptor 2; AQP, aquaporin; α -SMA, α -smooth-muscle-actin, ZO-1, zonula occludens-1; iNOS, inducible nitric oxide synthase; * $p < 0.05$ versus AL group

and induced autophagy. For the first time, our work demonstrated that CR attenuated glioma-induced brain edema, which might contribute to the prolonged survival.

The adrenal gland and particularly corticosterone levels have been shown to be important factors in the development of brain tumor growth and edema [22, 23]. Plasma corticosterone levels were found increased in the CR group compared to AL group. Thus, it is possible that the delay in tumor growth and attenuation of tumor edema might be due to increased levels of corticosterone observed in CR fed mice.

The crucial cause of brain tumor edema was the defect in the blood-tumor barrier. Increased vascular permeability in human brain tumors has been demonstrated by computed tomographic measurements of blood-tumor barrier permeability [24] and by immunohistochemical detection of plasma proteins in tumor parenchyma [25]. Most brain tumors including glioma over-secreted VEGF and over-expressed VEGFR2, which led to an abnormally permeable tumor vasculature, allowed fluid to leak from the intravascular space into the brain parenchyma, ultimately caused vasogenic cerebral edema [26]. Clinical and animals studies demonstrated the anti-edema effect through inhibiting VEGF/VEGFR2 signaling pathway [26, 27]. In this work, CR decreased serum VEGF content and suppressed tumor VEGF and VEGFR2 expression, which was similar with a precious report [11].

The leakiness of the blood-tumor barrier occurs primarily because of defects in interendothelial tight junctions. Occludin, claudin-1 and claudin-5 were found

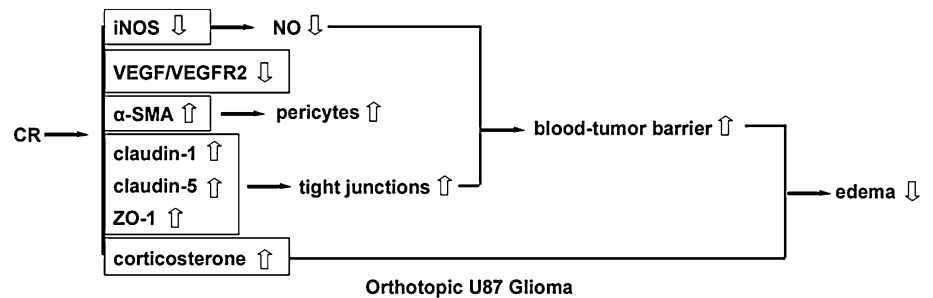
downregulated in human gliomas and metastatic tumor vessel [28, 29]. Recently, it was reported that dietary restriction of methionine, sulfur-containing amino acids, cysteine, and cystine improved tight junction barrier function [30, 31]. In this work, we first observed that CR enhanced proteins expression of claudin-1, claudin-5, and ZO-1 and improved tight junction in U87 gliomas.

In addition, CR enhanced α -smooth-muscle actin (α -SMA) expression, a marker of pericytes, in U87 gliomas. The instability of tumor blood vessels and leaky endothelial cell lining is associated with the absence of a surrounding sheath of α -SMA positive pericytes [32, 33]. Our result indicated that CR might enhance pericytes number surrounding endothelial cells to decrease vascular permeability in U87 gliomas.

NO is an unstable free radical gas and plays an important role in regulation of tumor permeability and cerebral edema. Yin et al. observed the augmentation of brain tumor permeability in glioma-bearing rats with nitric oxide donors [34]. The iNOS, a cell type-specific enzyme that catalyzed the synthesis of NO, was reported increased in the established gliomas [35]. Glioma tumorigenicity was decreased by iNOS knockout, indicating its role in progression of glioma [36]. Zanetti et al. found CR decreased iNOS expression in aged aorta [37]. In the current work, we found CR suppressed iNOS expression and reduced NO formation in U87 gliomas.

Several groups have proposed the involvement of aquaporins (AQPs) in the pathophysiology of brain edema [38–40]. Aquaporins form a superfamily of 13 members

Fig. 5 A schematic diagram illustrating the effect of CR on edema in U87 gliomas. iNOS, inducible nitric oxide synthase; NO, nitric oxide; VEGF, vascular endothelial growth factor; VEGFR2, vascular endothelial growth factor receptor 2; α -SMA, α -smooth-muscle-actin, ZO-1, zonula occludens-1



and are the principle pathway for water movement across most cellular membranes. Of these, AQP1 and AQP4 proteins were found highly expressed in the most malignant gliomas [41, 42]. In the current work, we found CR suppressed AQP1 protein expression in gliomas. Hayashi et al. found that induction of AQP1 expression in glioma correlated with the level of glycolysis, suggesting specific upregulation of AQP1 under glycolytic conditions [43]. Therefore, CR might suppress tumor AQP1 expression through modulating glycolysis. However, it was not known whether tumour-associated AQP1 was functional or whether it played a role in the pathophysiology of brain tumor edema. Further investigation was required.

A report from Kalaany and Sabatini revealed that U87-MG were resistant to dietary restriction [44]. The U87 tumor in the Kalaany and Sabatini study was grown in a non-orthotopic location (subcutaneous) and in the NOD/SCID (non-obese diabetic, severe combined immunodeficient) mouse host, which had characteristics of both type 1 and type 2 diabetes [45]. In our work, tumors were implanted in natural orthotopic site and in male athymic mice. The differences in growth site and mouse host strain might be responsible for the differences between our work and study of Kalaany and Sabatini. The underlying mechanism required further investigation.

Most previous reports about the effect of CR on gliomas focused on tumor growth. Different from them, we found that CR attenuated edema in U87 gliomas for the first time, which might contribute to its beneficial effect on the survival of glioma-bearing mice.

Finally, one limitation in the present work should be noted. We demonstrated that CR elevated serum corticosterone, suppressed expression of VEGF and VEGFR2, improved tight junctions, and suppressed inducible nitric oxide synthase (iNOS) expression and nitric oxide (NO) formation. However, we lacked direct evidence of causal effect between edema of glioma model and corticosterone, VEGF, tight junction, iNOS and NO formation, which required further investigation.

In conclusion, CR alleviated edema in a mouse U87 glioma model. Elevation of corticosterone, suppression of VEGF/VEGFR2, improvement of tight junctions, and suppression of iNOS expression and NO formation might

contribute to the beneficial effect of CR on edema in U87 gliomas (Fig. 5).

Ethical standards The experiments comply with the current laws of China.

Conflict of interest The authors declare that we have no conflict of interest.

References

- Stupp R, Hegi ME, Mason WP, Van den Bent MJ, Taphoorn MJ, Janzer RC, Ludwin SK, Allgeier A, Fisher B, Belanger K, Hau P, Brandes AA, Gijtenbeek J, Marosi C, Vecht CJ, Mokhtari K, Wesseling P, Villa S, Eisenhauer E, Gorlia T, Weller M, Lacombe D, Cairncross JG, Mirimanoff RO, European Organisation for Research and Treatment of Cancer Brain Tumour and Radiation Oncology Groups, National Cancer Institute of Canada Clinical Trials Group (2009) Effects of radiotherapy with concomitant and adjuvant temozolomide versus radiotherapy alone on survival in glioblastoma in a randomised phase III study: 5-year analysis of the EORTC-NCIC trial. *Lancet Oncol* 10:459–466
- Papadopoulos MC, Saadoun S, Davies DC, Bell BA (2001) Emerging molecular mechanisms of brain tumour oedema. *Br J Neurosurg* 15:101–108
- Marshall LF, King J, Langfitt TW (1977) The complications of high-dose corticosteroid therapy in neurosurgical patients: a prospective study. *Ann Neurol* 1:201–203
- Weissman DE, Dufer D, Vogel V, Abeloff MD (1987) Corticosteroid toxicity in neuro-oncology patients. *J Neurooncol* 5:125–128
- Tannenbaum A (1942) The genesis and growth of tumors. II. Effects of caloric restriction per se. *Cancer Res* 2:460–467
- Weindruch R, Walford RL, Fligiel S, Guthrie D (1986) The retardation of aging in mice by dietary restriction: longevity, cancer, immunity and lifetime energy intake. *J Nutr* 116:641–654
- Kritchevsky D (2002) Caloric restriction and experimental carcinogenesis. *Hybrid Hybridom* 21:147–151
- Seyfried TN, Kiebish MA, Marsh J, Shelton LM, Huysentruyt LC, Mukherjee P (2011) Metabolic management of brain cancer. *Biochim Biophys Acta* 1807:577–594
- Seyfried TN, Sanderson TM, El-Abbadi MM, McGowan R, Mukherjee P (2003) Role of glucose and ketone bodies in the metabolic control of experimental brain cancer. *Br J Cancer* 89:1375–1382
- Urits I, Mukherjee P, Meidenbauer J, Seyfried TN (2012) Dietary restriction promotes vessel maturation in a mouse astrocytoma. *J Oncol* 2012:264039

11. Mukherjee P, Abate LE, Seyfried TN (2004) Antiangiogenic and proapoptotic effects of dietary restriction on experimental mouse and human brain tumors. *Clin Cancer Res* 10:5622–5629
12. Marsh J, Mukherjee P, Seyfried TN (2008) Akt-dependent proapoptotic effects of dietary restriction on late-stage management of a phosphatase and tensin homologue/tuberous sclerosis complex 2-deficient mouse astrocytoma. *Clin Cancer Res* 14:7751–7762
13. Shelton LM, Huysentruyt LC, Mukherjee P, Seyfried TN (2010) Calorie restriction as an anti-invasive therapy for malignant brain cancer in the VM mouse. *ASN Neuro* 2:e00038
14. Raney MK, El-Abbadi M, Manfredi MG, Mukherjee P, Platt FM, Seyfried TN (2001) N-butyldeoxyjirimycin reduces growth and ganglioside content of experimental mouse brain tumours. *Br J Cancer* 84:1107–1114
15. Groothuis DR, Fischer JM, Pasternak JF, Blasberg RG, Vick NA, Bigner DD (1983) Regional measurements of blood-to-tissue transport in experimental RG-2 rat gliomas. *Cancer Res* 43:3368–3373
16. Nomura T, Inamura T, Black KL (1994) Intracarotid infusion of bradykinin selectively increases blood-tumor permeability in 9L and C6 brain tumors. *Brain Res* 659:62–66
17. Zhou W, Mukherjee P, Kiebish MA, Markis WT, Mantis JG, Seyfried TN (2007) The calorically restricted ketogenic diet, an effective alternative therapy for malignant brain cancer. *Nutr Metab* 4:5
18. Nebeling LC, Miraldi F, Shurin SB, Lerner E (1995) Effects of a ketogenic diet on tumor metabolism and nutritional status in pediatric oncology patients: two case reports. *J Am Coll Nutr* 14:202–208
19. Ruggeri BA, Klurfeld DM, Kritchevsky D (1987) Biochemical alterations in 7,12-dimethylbenz[a]anthracene-induced mammary tumors from rats subjected to caloric restriction. *Biochim Biophys Acta* 929:239–246
20. Roslin M, Henriksson R, Bergstrom P, Ungerstedt U, Bergenheim AT (2003) Baseline levels of glucose metabolites, glutamate and glycerol in malignant glioma assessed by stereotactic microdialysis. *J Neuro-oncol* 61:151–160
21. Oudard S, Boitier E, Miccoli L, Rousset S, Dutrillaux B, Poupon MF (1997) Gliomas are driven by glycolysis: putative roles of hexokinase, oxidative phosphorylation and mitochondrial ultrastructure. *Anticancer Res* 17:1903–1911
22. Galicich JH, French LA, Melby JC (1961) Use of dexamethasone in treatment of cerebral edema associated with brain tumors. *J Lancet* 81:46–53
23. Pashko LL, Schwartz AG (1992) Reversal of food restriction-induced inhibition of mouse skin tumor promotion by adrenalectomy. *Carcinogenesis* 13:1925–1928
24. Groothuis DR, Lapin GD, Vriesendorp FJ, Mikhael MA, Patlak CS (1991) A method to quantitatively measure transcapillary transport of iodinated compounds in canine brain tumors with computed tomography. *J Cereb Blood Flow Metab* 11:939–948
25. Seitz RJ, Wechsler W (1987) Immunohistochemical demonstration of serum proteins in human cerebral gliomas. *Acta Neuropathol (Berl)* 73:145–152
26. Gerstner ER, Duda DG, di Tomaso E, Ryg PA, Loeffler JS, Sorensen AG, Ivy P, Jain RK, Batchelor TT (2009) VEGF inhibitors in the treatment of cerebral edema in patients with brain cancer. *Nat Rev Clin Oncol* 6:229–236
27. Kamoun WS, Ley CD, Farrar CT, Duyverman AM, Lahdenranta J, Lacorre DA, Batchelor TT, di Tomaso E, Duda DG, Munn LL, Fukumura D, Sorensen AG, Jain RK (2009) Edema control by cediranib, a vascular endothelial growth factor receptor-targeted kinase inhibitor, prolongs survival despite persistent brain tumor growth in mice. *J Clin Oncol* 27:2542–2552
28. Lee J, Baird A, Eliceiri BP (2011) In vivo measurement of glioma-induced vascular permeability. *Methods Mol Biol* 763:417–422
29. Rascher G, Fischmann A, Kroger S, Duffner F, Grote EH, Wolburg H (2002) Extracellular matrix and the blood-brain barrier in glioblastoma multiforme: spatial segregation of tenascin and agrin. *Acta Neuropathol (Berl)* 104:85–91
30. Ramalingam A, Wang X, Gabello M, Valenzano MC, Soler AP, Ko A, Morin PJ, Mullin JM (2010) Dietary methionine restriction improves colon tight junction barrier function and alters claudin expression pattern. *Am J Physiol Cell Physiol* 299:C1028–C1035
31. Mullin JM, Skrovanek SM, Valenzano MC (2009) Modification of tight junction structure and permeability by nutritional means. *Ann N Y Acad Sci* 1165:99–112
32. Verbeek MM, Otte-Höller I, Wesseling P, Ruiter DJ, de Waal RM (1994) Induction of alpha-smooth muscle actin expression in cultured human brain pericytes by transforming growth factor-beta 1. *Am J Pathol* 144:372–382
33. De Bock K, Cauwenberghs S, Carmeliet P (2011) Vessel abnormalization: another hallmark of cancer? Molecular mechanisms and therapeutic implications. *Curr Opin Genet Dev* 21:73–79
34. Yin D, Wang X, Konda BM, Ong JM, Hu J, Sacapano MR, Ko MK, Espinoza AJ, Irvin DK, Shu Y, Black KL (2008) Increase in brain tumor permeability in glioma-bearing rats with nitric oxide donors. *Clin Cancer Res* 14:4002–4009
35. Kostourou V, Cartwright JE, Johnstone AP, Boulton JK, Cullis ER, Whitley G, Robinson SP (2011) The role of tumour-derived iNOS in tumour progression and angiogenesis. *Br J Cancer* 104:83–90
36. Yamaguchi S, Bell HS, Shinoda J, Holmes MC, Wharton SB, Whittle IR (2002) Glioma tumorigenicity is decreased by iNOS knockout: experimental studies using the C6 striatal implantation glioma model. *Br J Neurosurg* 16:567–572
37. Zanetti M, Gortan Cappellari G, Burekovic I, Barazzoni R, Stebel M, Guarnieri G (2010) Caloric restriction improves endothelial dysfunction during vascular aging: effects on nitric oxide synthase isoforms and oxidative stress in rat aorta. *Exp Gerontol* 45:848–855
38. Venero JL, Vizuete ML, Machado A, Cano J (2001) Aquaporins in the central nervous system. *Prog Neurobiol* 63:321–336
39. Agre P, Kozono D (2003) Aquaporin water channels: molecular mechanisms for human diseases. *FEBS Lett* 555:72–78
40. Papadopoulos MC, Krishna S, Verkman AS (2002) Aquaporin water channels and brain edema. *Mt Sinai J Med* 69:242–248
41. Saadoun S, Papadopoulos MC, Davies DC, Bell BA, Krishna S (2002) Increased aquaporin 1 water channel expression in human brain tumours. *Br J Cancer* 87:621–623
42. Saadoun S, Papadopoulos MC, Davies DC, Krishna S, Bell BA (2002) Aquaporin-4 expression is increased in oedematous human brain tumours. *J Neurol Neurosurg Psychiatry* 72:262–265
43. Hayashi Y, Edwards NA, Proescholdt MA, Oldfield EH, Merrill MJ (2007) Regulation and function of aquaporin-1 in glioma cells. *Neoplasia* 9:777–787
44. Kalaany NY, Sabatini DM (2009) Tumours with PI3K activation are resistant to dietary restriction. *Nature* 458:725–731
45. Chaparro RJ, Konigshofer Y, Beilhack GF, Shizuru JA, McDevitt HO, Chien YH (2006) Nonobese diabetic mice express aspects of both type 1 and type 2 diabetes. *Proc Natl Acad Sci USA* 103:12475–12480